PHYSICAL REVIEW C **86**, 031601(R) (2012)

Effects of four-body breakup on ^{6}Li elastic scattering near the Coulomb barrier

Shin Watanabe,[1,*] Takuma Matsumoto,[1,†] Kosho Minomo,[1,‡] Kazuyuki Ogata,[2,§] and Masanobu Yahiro[1,‖]
[1]*Department of Physics, Kyushu University, Fukuoka 812-8581, Japan*
[2]*Research Center for Nuclear Physics (RCNP), Osaka University, Ibaraki 567-0047, Japan*
(Received 15 May 2012; revised manuscript received 25 August 2012; published 25 September 2012)

We investigate projectile breakup effects on ^{6}Li + ^{209}Bi elastic scattering near the Coulomb barrier with the four-body version of the continuum-discretized coupled-channels method (four-body CDCC). The elastic scattering is well described by the $p + n + {}^4$He + ^{209}Bi four-body model. Furthermore, we propose a reasonable $d + {}^4$He + ^{209}Bi three-body model for describing the four-body scattering, clarifying four-body dynamics of the elastic scattering.

DOI: 10.1103/PhysRevC.86.031601 PACS number(s): 24.10.Eq, 25.60.Gc, 25.60.Bx

Introduction. Plenty of nuclei are considered to have two-cluster or three-cluster configurations as their main components. Three-cluster dynamics is, however, nontrivial compared with two-cluster dynamics. Systematic understanding of three-cluster dynamics is hence important. There are many nuclei that can be described by three-cluster models. For example, low-lying states of ^{6}He and ^{6}Li are explained by $N + N + {}^4$He three-body models [1–6], where N stands for a nucleon. The comparison of the two nuclei is important to see the difference between dineutron and proton-neutron correlations. Two-neutron halo nuclei such as ^{11}Li, ^{14}Be, and ^{22}C are reasonably described by a $n + n + X$ three-cluster model, where X is a core nucleus. Properties of these three-cluster configurations should be confirmed by measuring scattering of the nuclei and analyzing the measured cross sections with accurate reaction theories. The reactions are essentially four-body scattering composed of three constituents of the projectile and a target nucleus. An accurate theoretical description of four-body scattering is thus an important subject in nuclear physics.

The continuum-discretized coupled-channels method (CDCC) is a fully quantum mechanical method of describing not only three-body scattering but also four-body scattering [7–9]. CDCC has succeeded in reproducing experimental data on both three- and four-body scattering. The theoretical foundation of CDCC is shown with the distorted Faddeev equation [10–12]. CDCC for four-body (three-body) scattering is often called four-body (three-body) CDCC; see Refs. [13–25] and references therein for four-body CDCC. So far four-body CDCC has been applied to only ^{6}He scattering.

For ^{6}He + ^{209}Bi scattering at 19 and 22.5 MeV near the Coulomb barrier, the measured total reaction cross sections are largely enhanced in comparison with that for ^{6}Li + ^{209}Bi scattering at 29.9 and 32.8 MeV near the Coulomb barrier [26,27]. Keeley *et al.* [28] analyzed the ^{6}He + ^{209}Bi scattering with three-body CDCC in which the ^{6}He + ^{209}Bi system was assumed to be a $^2n + {}^4$He + ^{209}Bi three-body system; i.e., a pair of extra neutrons in ^{6}He was treated as a single particle, a dineutron (^2n). The enhancement of the total reaction cross section of ^{6}He + ^{209}Bi scattering is found to be due to the electric dipole ($E1$) excitation of ^{6}He to its continuum states [29], i.e., Coulomb breakup of ^{6}He. The three-body CDCC calculation, however, does not reproduce the angular distribution of the measured elastic cross section and overestimates the measured total reaction cross section by a factor of 2.5. This problem is solved by four-body CDCC [19] in which the total system is assumed to be a $n + n + {}^4$He + ^{209}Bi four-body system.

^{6}Li + ^{209}Bi scattering near the Coulomb barrier was, meanwhile, analyzed with three-body CDCC by assuming a $d + {}^4$He + ^{209}Bi three-body model [28]. The three-body CDCC calculation could not reproduce the data without normalization factors for the potentials between ^{6}Li and ^{209}Bi. This result indicates that four-body CDCC should be applied to ^{6}Li + ^{209}Bi scattering.

In this Rapid Communication, we analyze ^{6}Li + ^{209}Bi elastic scattering at 29.9 and 32.8 MeV with four-body CDCC by assuming the $p + n + {}^4$He + ^{209}Bi four-body model. The four-body CDCC calculation reproduces the measured elastic cross sections, whereas the previous three-body CDCC calculation does not. Four-body dynamics of the elastic scattering is investigated, and what causes the failure of the previous three-body CDCC calculation is discussed. Finally, we propose a reasonable $d + {}^4$He + ^{209}Bi three-body model for describing the four-body scattering.

Theoretical framework. One of the most natural frameworks to describe ^{6}Li + ^{209}Bi scattering is the $p + n + {}^4$He + ^{209}Bi four-body model. The dynamics of the scattering is governed by the Schrödinger equation

$$(H - E)\Psi = 0 \tag{1}$$

for the total wave function Ψ, where E is a total energy of the system. The total Hamiltonian H is defined by

$$H = K_R + U + h \tag{2}$$

with

$$U = U_n(R_n) + U_p(R_p) + U_\alpha(R_\alpha) + \frac{e^2 Z_{\rm Li} Z_{\rm Bi}}{R}, \tag{3}$$

*s-watanabe@phys.kyushu-u.ac.jp
†matsumoto@phys.kyushu-u.ac.jp
‡minomo@phys.kyushu-u.ac.jp
§kazuyuki@rcnp.osaka-u.ac.jp
‖yahiro@phys.kyushu-u.ac.jp

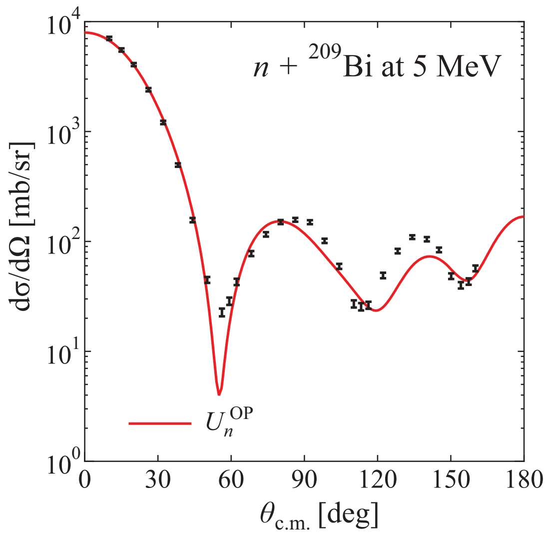

FIG. 1. (Color online) Angular distribution of elastic cross section for $n + {}^{209}$Bi scattering at 5 MeV. The solid line is the result with the neutron optical potential $U_n^{\rm OP}$. The experimental data are taken from Ref. [31].

where h denotes the internal Hamiltonian of ^{6}Li, $\boldsymbol{R}$ is the center-of-mass coordinate of ^{6}Li relative to ^{209}Bi, K_R stands for the kinetic energy operator associated with $\boldsymbol{R}$, and U_x describes the nuclear part of the optical potential between x and ^{209}Bi as a function of the relative coordinate R_x. As U_α, we adopt the optical potential of Barnett and Lilley [30]. The parameters of U_n are fitted to reproduce experimental data [31] on $n + {}^{209}$Bi elastic scattering at 5 MeV, where only the central interaction is taken for simplicity. As shown in Fig. 1, the neutron optical potential $U_n^{\rm OP}$ thus fitted is consistent with the data. The resultant parameter set is the same as that in the global optical potential of Koning and Delaroche [32], except that parameters a_V, W_V, and W_D are changed into 0.55 fm, 0 MeV, and 4.0 MeV, respectively. The proton optical potential U_p is assumed to be the same as U_n.

In the $d + {}^4$He two-cluster model, the dipole strength of ^{6}Li is zero, since the mass ratio between the two clusters is equal to the charge ratio between them. In the $n + p + {}^4$He three-cluster model, we have confirmed numerically that the dipole strength is still negligibly small, because the ^{6}Li ground state is dominated by the $d + {}^4$He component. This property strongly suppresses Coulomb breakup processes in ^{6}Li-^{209}Bi scattering. Hence we can approximate the Coulomb part of p-^{209}Bi and α-^{209}Bi interactions as $e^2 Z_{\rm Li} Z_{\rm Bi}/R$, as shown in Eq. (3), where $Z_{\rm A}$ is the atomic number of the nucleus A.

The internal Hamiltonian h of ^{6}Li is described by the $p + n + {}^4$He orthogonality condition model [33]. The Hamiltonian of ^{6}Li agrees with that of ^{6}He in Ref. [19], when the Coulomb interaction between p and ^{4}He is neglected. Namely, the Bonn-A interaction [34] is taken in the p-n subsystem and the so-called KKNN interaction [35] is used in the p-α and n-α subsystems, where the KKNN interaction is determined from experimental data on low-energy nucleon-α scattering. In order to reproduce the measured binding energy of ^{6}Li, we

TABLE I. Calculated spin-parity (I^π), energy (ϵ_0), and matter radius ($R^{\rm m}_{\rm rms}$) of the ^{6}Li ground state. The experimental data are taken from Refs. [36,37].

	I^π	ϵ_0 (MeV)	$R^{\rm m}_{\rm rms}$ (fm)
Calc.	1^+	−3.68	2.34
Exp.	1^+	−3.6989	2.44 ± 0.07

introduce the effective three-body interaction defined by

$$V^{\rm 3body}(y_1, y_2) = V_3 e^{-\nu(y_1^2+y_2^2)}, \tag{4}$$

where $\boldsymbol{y}_1$ ($\boldsymbol{y}_2$) is the relative coordinate between a valence neutron (proton) and ^{4}He. The optimum values of V_3 and ν are −5.1 MeV and 0.1 fm^{-2}, respectively. The calculated results for the ^{6}Li ground state are summarized in Table I.

Eigenstates of h consist of a finite number of discrete states with negative energies and continuum states with positive energies. In four-body CDCC, the continuum states of the projectile are discretized into a finite number of pseudostates by either the pseudostate method [13–21,23–25] or the momentum-bin method [22]. The Schrödinger equation (1) is solved in a model space $\mathcal{P}$ spanned by the discrete and discretized-continuum states:

$$\mathcal{P}(H-E)\mathcal{P}\Psi_{\rm CDCC} = 0. \tag{5}$$

In the pseudostate method, the discrete and discretized-continuum states are obtained by diagonalizing h in a space spanned by L^2-type basis functions. As the basis function, the Gaussian [14–16,19,23–25] or the transformed harmonic oscillator function [13,17,18,20,21] is usually taken. In this paper, we use the Gaussian function. The model space $\mathcal{P}$ is then described by

$$\mathcal{P} = \sum_{nIm} |\Phi_{nIm}\rangle\langle\Phi_{nIm}|, \tag{6}$$

where Φ_{nIm} is the nth eigenstate of ^{6}Li with an energy ϵ_{nI}, a total spin I, and its projection on the z axis, m.

The CDCC wave function $\Psi^{JM}_{\rm CDCC}$, with total angular momentum J and its projection on the z axis, M, is expressed as

$$\Psi^{JM} = \sum_{\gamma} \chi^J_\gamma(P_{nI}, R)/R\, \mathcal{Y}^{JM}_\gamma \tag{7}$$

with

$$\mathcal{Y}^{JM}_\gamma = [\Phi_{nI}(\boldsymbol{\xi}) \otimes i^L Y_L(\hat{\boldsymbol{R}})]_{JM} \tag{8}$$

for the orbital angular momentum L with respect to $\boldsymbol{R}$. Here $\boldsymbol{\xi}$ is a set of internal coordinates of ^{6}Li and the expansion coefficient χ^J_γ, where $\gamma = (n, I, L)$, describes a motion of ^{6}Li in its (n, I) state with linear momentum P_{nI} relative to the target. Multiplying the four-body Schrödinger equation (5) by $\mathcal{Y}^{*JM}_{\gamma'}$ from the left and integrating it over all variables except R, one can obtain a set of coupled differential equations for χ^J_γ:

$$\left[\frac{d^2}{dR^2} - \frac{L(L+1)}{R^2} - \frac{2\mu}{\hbar^2}U_{\gamma\gamma}(R) + P^2_{nI}\right]\chi^J_\gamma(P_{nI}, R) = \frac{2\mu}{\hbar^2}\sum_{\gamma'\neq\gamma} U_{\gamma'\gamma}(R)\chi^J_{\gamma'}(P_{n'I'}, R) \tag{9}$$

with the coupling potentials

$$U_{\gamma'\gamma}(R) = \langle \mathcal{Y}^{JM}_{\gamma'} | U_n(R_n) + U_p(R_p) + U_\alpha(R_\alpha) | \mathcal{Y}^{JM}_{\gamma} \rangle + \frac{e^2 Z_{\rm Li} Z_{\rm Bi}}{R} \delta_{\gamma'\gamma},$$

where μ is the reduced mass between ^{6}Li and ^{209}Bi. The elastic and discrete breakup S-matrix elements are obtained by solving Eq. (9) under the standard asymptotic boundary condition [7,38].

In order to obtain Φ_{nIm}, we assume $I^\pi = 1^+$, 2^+, and 3^+ states with isospin zero and diagonalize h with 10 Gaussian basis functions for each coordinate in which the range parameters are taken from 0.1 to 12 fm in a geometric series. As shown in Table I, the calculated binding energy and the matter radius of the ^{6}Li ground state are in good agreement with the experimental data. The Φ_{nIm} with its eigenenergy $\epsilon_{nI} > 20$ MeV are excluded from $\mathcal{P}$. The resulting numbers of discrete states are 64 (including the ground state of ^{6}Li), 56, and 57 for 1^+, 2^+, and 3^+ states, respectively. We have also confirmed numerically that other spin-parity states such as $I^\pi = 0^+$ and negative-parity states do not affect the present results. The model space thus obtained gives good convergence within 1% of the calculated elastic cross sections for the ^{6}Li + ^{209}Bi scattering at 29.9 and 32.8 MeV.

We also perform three-body CDCC calculations by assuming a d + ^{4}He + ^{209}Bi model, following Refs. [28,29]. As an interaction between d and ^{4}He, we take the potential of Ref. [39], which was determined from experimental data on the ground-state energy (-1.47 MeV) and the 3^+-resonance state energy (0.71 MeV) of ^{6}Li and low-energy d-α scattering phase shifts. The continuum states between d and ^{4}He are discretized with the pseudostate method [14] and are truncated at 20 MeV in the excitation energy of ^{6}Li from the d-^{4}He threshold. The d-^{209}Bi optical potential ($U_d^{\rm OP}$) [40] is taken as U_d, i.e., the distorting potential between d and ^{209}Bi in a d + ^{4}He + ^{209}Bi three-body Hamiltonian, whereas U_α is common between three- and four-body CDCC calculations.

Results. Figure 2 shows the angular distribution of elastic cross section for ^{6}Li + ^{209}Bi scattering at 29.9 MeV. The dotted line shows the result of three-body CDCC calculations with $U_d^{\rm OP}$ as U_d. This result underestimates the measured cross section [26,27]. The solid (dashed) line, meanwhile, stands for the result of four-body CDCC calculations with (without) projectile breakup effects. In CDCC calculations without ^{6}Li breakup, the model space $\mathcal{P}$ is composed only of the ^{6}Li ground state. The solid line reproduces the experimental cross section, but the dashed line does not. The projectile breakup effects are thus significant and the present ^{6}Li scattering is well described by the $p + n + {}^4$He + ^{209}Bi four-body model. This conclusion is true also for ^{6}Li + ^{209}Bi scattering at 32.8 MeV, as shown in Fig. 3.

Now we consider d breakup in the ^{6}Li scattering in order to understand four-body dynamics of the scattering. In the limit of no d breakup, the interaction between d and ^{209}Bi can be obtained by folding U_n and U_p with the deuteron density. This potential is referred to as the single-folding potential $U_d^{\rm SF}$. In Figs. 2 and 3, the dot-dashed lines show the results of three-body CDCC calculations with $U_d^{\rm SF}$ as U_d. The results well simulate those of four-body CDCC calculations, i.e., the solid lines. This indicates that d breakup is suppressed in ^{6}Li scattering. An intuitive understanding of this property is as follows. As a characteristic of the present ^{6}Li scattering, it is quite peripheral in virtue of the Coulomb barrier. The scattering is dominated by the configuration in which α is located between d and the target, because U_α is more attractive than U_d. In this configuration, d is out of the range of U_n and U_p, so that d breakup is suppressed. The ^{6}Li elastic scattering near the Coulomb barrier is thus well described by the d + α + ^{209}Bi three-body model, if $U_d^{\rm SF}$ is taken as U_d.

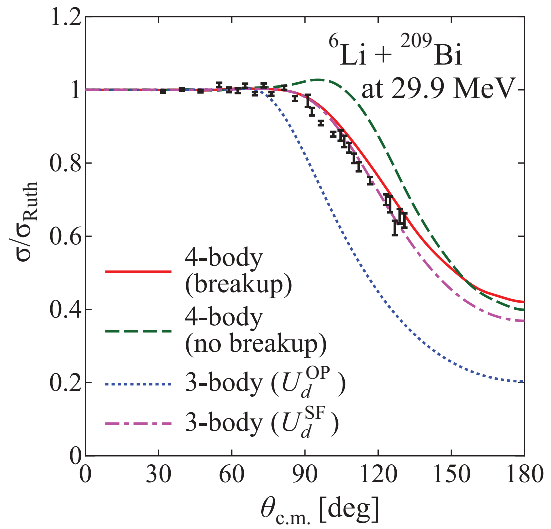

FIG. 2. (Color online) Angular distribution of the elastic cross section for ^{6}Li + ^{209}Bi scattering at 29.9 MeV. The cross section is normalized by the Rutherford cross section. The dotted (dot-dashed) line stands for the result of three-body CDCC calculations in which $U_d^{\rm OP}$ ($U_d^{\rm SF}$) is taken as U_d. The solid (dashed) line represents the result of four-body CDCC calculations with (without) breakup effects. The experimental data are taken from Refs. [26,27].

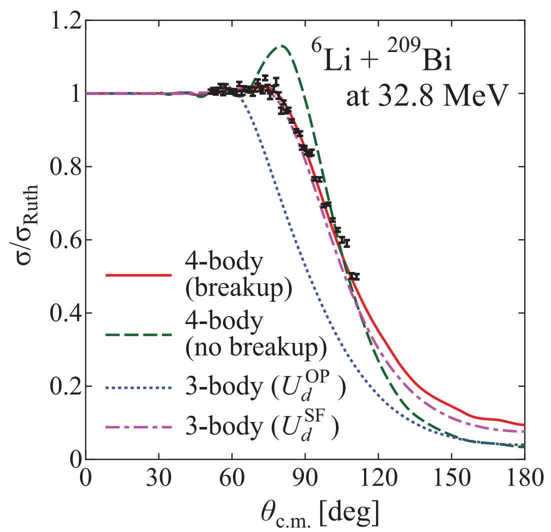

FIG. 3. (Color online) Same as in Fig. 2 but for ^{6}Li + ^{209}Bi scattering at 32.8 MeV.

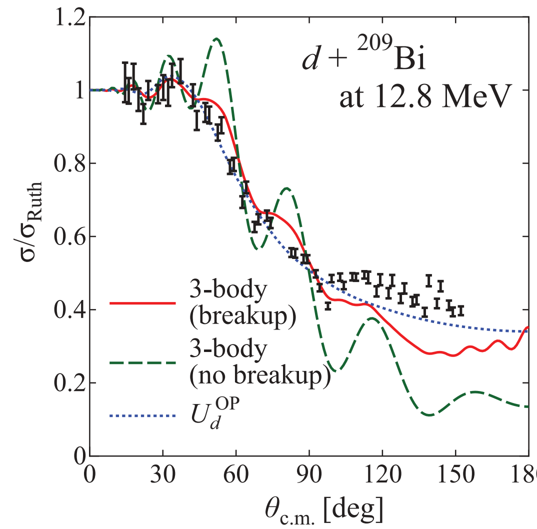

FIG. 4. (Color online) Angular distribution of the elastic cross section for $d + {}^{209}$Bi scattering at 12.8 MeV. The solid (dashed) line stands for the result of three-body CDCC calculations with (without) deuteron breakup, whereas the dotted line is the result of the deuteron optical potential U_d^{OP}. The experimental data are taken from Ref. [40].

Figure 4 shows the angular distribution of elastic cross section for $d + {}^{209}$Bi scattering at 12.8 MeV. The solid and dashed lines stand for the results of three-body CDCC calculations with and without d breakup, respectively, in which the $p + n + {}^{209}$Bi model is assumed and both Coulomb and nuclear breakup effects are taken into account. In this calculation, the discretized-continuum states of d, obtained by the pseudostate method, are truncated at 30 MeV in the excitation energy from the n-p threshold. As the relative angular momentum ℓ between n and p, we take up to $\ell = 4$. The resulting number of discretized states is 13 (14) for $\ell = 0$ and 1 ($\ell = 2$, 3, and 4). The model space gives good convergence of the calculated elastic cross sections within 1%. The solid line reproduces the data fairly well, but the dashed line does not. Thus d breakup is significant for deuteron scattering. The deuteron optical potential U_d^{OP} (dotted line) yields fairly good agreement with the data, but the radius of U_d^{OP} is larger than that of U_d^{SF}. This is the reason why three-body CDCC calculations with U_d^{OP} as U_d cannot reproduce the measured elastic cross section for ^{6}Li + ^{209}Bi scattering. The difference between U_d^{SF} and U_d^{OP} mainly comes from the fact that U_d^{OP} includes d-breakup effects, whereas U_d^{SF} does not.

Summary. ^{6}Li + ^{209}Bi scattering at 29.9 and 32.8 MeV near the Coulomb barrier is well described by four-body CDCC based on the $p + n + {}^4$He + ^{209}Bi model. In ^{6}Li scattering, d breakup is strongly suppressed, suggesting that the $d + {}^4$He + ^{209}Bi model becomes good, if the single-folding potential U_d^{SF} with no d breakup is taken as an interaction between d and the target. For $d + {}^{209}$Bi scattering at 12.8 MeV, meanwhile, d breakup is significant, so that the deuteron optical potential U_d^{OP} includes d-breakup effects.

Four-body CDCC is applicable also for $n + {}^6$Li scattering, which is a key reaction in nuclear engineering. In the scattering, ^{6}Li breakup into $n + p + \alpha$ is considered to be not negligible for emitted neutron spectra [41]. We will discuss this point in a forthcoming paper.

The authors would like to thank Y. Watanabe and K. Katō for helpful discussions. This work has been supported in part by the Grants-in-Aid for Scientific Research of Monbukagakusho of Japan and JSPS.

[1] S. Funada, H. Kameyama, and Y. Sakuragi, Nucl. Phys. A **575**, 93 (1994).
[2] E. Hiyama and M. Kamimura, Nucl. Phys. A **588**, c35 (1995).
[3] T. Myo, K. Katō, S. Aoyama, and K. Ikeda, Phys. Rev. C **63**, 054313 (2001).
[4] A. Csótó, Phys. Rev. C **49**, 3035 (1994).
[5] K. Arai, Y. Suzuki, and K. Varga, Phys. Rev. C **51**, 2488 (1995).
[6] Y. Kikuchi, N. Kurihara, A. Wano, K. Katō, T. Myo, and M. Takashina, Phys. Rev. C **84**, 064610 (2011).
[7] M. Kamimura, M. Yahiro, Y. Iseri, Y. Sakuragi, H. Kameyama, and M. Kawai, Prog. Theor. Phys. Suppl. **89**, 1 (1986).
[8] N. Austern, Y. Iseri, M. Kamimura, M. Kawai, G. Rawitscher, and M. Yahiro, Phys. Rep. **154**, 125 (1987).
[9] M. Yahiro, K. Ogata, T. Matsumoto, and K. Minomo, Prog. Theor. Exp. Phys. **2012**, 01A206 (2012).
[10] N. Austern, M. Yahiro, and M. Kawai, Phys. Rev. Lett. **63**, 2649 (1989).
[11] N. Austern, M. Kawai, and M. Yahiro, Phys. Rev. C **53**, 314 (1996).
[12] A. Deltuva, A. M. Moro, E. Cravo, F. M. Nunes, and A. C. Fonseca, Phys. Rev. C **76**, 064602 (2007).
[13] A. M. Moro, J. M. Arias, J. Gómez-Camacho, I. Martel, F. Pérez-Bernal, R. Crespo, and F. Nunes, Phys. Rev. C **65**, 011602(R) (2001).
[14] T. Matsumoto, T. Kamizato, K. Ogata, Y. Iseri, E. Hiyama, M. Kamimura, and M. Yahiro, Phys. Rev. C **68**, 064607 (2003).
[15] T. Matsumoto, E. Hiyama, K. Ogata, Y. Iseri, M. Kamimura, S. Chiba, and M. Yahiro, Phys. Rev. C **70**, 061601(R) (2004).
[16] T. Egami, K. Ogata, T. Matsumoto, Y. Iseri, M. Kamimura, and M. Yahiro, Phys. Rev. C **70**, 047604 (2004).
[17] M. Rodríguez-Gallardo, J. M. Arias, J. Gómez-Camacho, A. M. Moro, I. J. Thompson, and J. A. Tostevin, Phys. Rev. C **72**, 024007 (2005).
[18] A. M. Moro, F. Pérez-Bernal, J. M. Arias, and J. Gómez-Camacho, Phys. Rev. C **73**, 044612 (2006).
[19] T. Matsumoto, T. Egami, K. Ogata, Y. Iseri, M. Kamimura, and M. Yahiro, Phys. Rev. C **73**, 051602(R) (2006).
[20] M. Rodríguez-Gallardo, J. M. Arias, J. Gómez-Camacho, R. C. Johnson, A. M. Moro, I. J. Thompson, and J. A. Tostevin, Phys. Rev. C **77**, 064609 (2008).
[21] A. M. Moro, J. M. Arias, J. Gómez-Camacho, and F. Pérez-Bernal, Phys. Rev. C **80**, 054605 (2009).
[22] M. Rodríguez-Gallardo, J. M. Arias, J. Gómez-Camacho, A. M. Moro, I. J. Thompson, and J. A. Tostevin, Phys. Rev. C **80**, 051601(R) (2009).
[23] T. Egami, T. Matsumoto, K. Ogata, and M. Yahiro, Prog. Theor. Phys. **121**, 789 (2009).

[24] T. Matsumoto, T. Egami, K. Ogata, and M. Yahiro, Prog. Theor. Phys. **121**, 885 (2009).
[25] T. Matsumoto, K. Katō, and M. Yahiro, Phys. Rev. C **82**, 051602(R) (2010).
[26] E. F. Aguilera *et al.*, Phys. Rev. Lett. **84**, 5058 (2000).
[27] E. F. Aguilera *et al.*, Phys. Rev. C **63**, 061603 (2001).
[28] N. Keeley, J. M. Cook, K. W. Kemper, B. T. Roeder, W. D. Weintraub, F. Maréchal, and K. Rusek, Phys. Rev. C **68**, 054601 (2003).
[29] K. Rusek, I. Martel, J. Gómez-Camacho, A. M. Moro, and R. Raabe, Phys. Rev. C **72**, 037603 (2005).
[30] A. R. Barnett and J. S. Lilley, Phys. Rev. C **9**, 2010 (1974).
[31] J. Annand, R. Finlay, and P. Dietrich, Nucl. Phys. A **443**, 249 (1985).
[32] A. J. Koning and J. P. Delaroche, Nucl. Phys. A **713**, 231 (2003).
[33] S. Saito, Prog. Theor. Phys. **41**, 705 (1969).
[34] R. Machleidt, Adv. Nucl. Phys. **19**, 189 (1989).
[35] H. Kanada, T. Kaneko, S. Nagata, and M. Nomoto, Prog. Theor. Phys. **61**, 1327 (1979).
[36] D. R. Tilley *et al.*, Nucl. Phys. A **708**, 3 (2002).
[37] A. V. Dobrovolsky *et al.*, Nucl. Phys. A **766**, 1 (2006).
[38] R. A. D. Piyadasa, M. Yahiro, M. Kamimura, and M. Kawai, Prog. Theor. Phys. **81**, 910 (1989).
[39] Y. Sakuragi, M. Yahiro, and M. Kamimura, Prog. Theor. Phys. Suppl. **89**, 136 (1986).
[40] A. Budzanowski, L. Freindl, K. Grotowski, M. Rzeszutko, M. Słapa, J. Szmider, and P. Hodgson, Nucl. Phys. **49**, 144 (1963).
[41] T. Matsumoto, D. Ichinkhorloo, Y. Hirabayashi, K. Katō, and S. Chiba, Phys. Rev. C **83**, 064611 (2011).